PAPER

The effect of thermal expansion on photoisomerisation in the crystals of [Co(NH₃)₅NO₂]Cl(NO₃): different strain origins – different outcomes†

A. A. Sidelnikov,*[a] S. A. Chizhik,[a] B. A. Zakharov,[ab] A. P. Chupakhin[b] and E. V. Boldyreva[a]

The effect of anisotropic structural strain resulting from thermal expansion on linkage photoisomerisation in crystals of [Co(NH₃)₅NO₂]Cl(NO₃) was studied. The quantum yield of the photoisomerisation was qualitatively correlated with the bending of needle-shaped crystals across a series of temperatures from 80–363 K. The thermal evolution of the crystal structure was also studied across the same temperature range by single-crystal X-ray diffraction. A qualitative correlation was found between the photo-reaction rate and both the cell volume and the volume of void space around the nitro groups. However, this correlation was found to be non-linear. The effect of the anisotropic structural strain resulting from temperature variations on the rate of photoisomerisation is qualitatively different from the effect of strain that is generated by elastic external loading. If strain is induced by external load, the reaction rate correlates linearly with compression along the crystallographic *b* direction. In contrast, if strain results from temperature variations, then the reaction rate correlates linearly with changes along the crystallographic *a* direction. This effect is measured quantitatively and its rationalisation is attempted.

Introduction

Photomechanical effects in molecular crystals have been studied since the 1980s,[1–3] and interest in these phenomena increases every year.[4–10] One of the most spectacular manifestations of photomechanical effects is the bending of crystals on irradiation, which was first reported in the 1980s (ref. 1–3) and has since been reproduced many times for a variety of compounds (see recent reviews[4–10]).

Crystals of [Co(NH₃)₅NO₂]Cl(NO₃) belong to the most extensively studied compounds that exhibit photomechanical effects, namely bend or jump on homogeneous nitro–nitrito intramolecular linkage isomerisation (the nitro-ligand changes its coordination to the Co(III)-atom from nitrogen in the nitro-form to oxygen in the nitrito-isomer):[2,11–16]
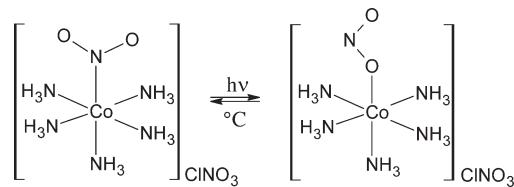
They can be grown as long thin needles, making it possible to monitor the photoisomerisation quantitatively by precise measurements of crystal bending.[2,9,13,17,18] Photochemical transformation is directly related to macroscopic crystal deformation, making it possible to study the microscopic mechanism of the photo-transformation from the macroscopic mechanical response.[9] Measuring crystal bending has been used to study the effect of the elastic compression of crystals along axis *b* induced by external load on the quantum yield of the photoisomerisation; in this way the activation volume has been estimated.[11,13,17,18] Although a change in the molar volume over the course of the nitro–nitrito photoisomerisation is negative (the volume is reduced),[19] the activation volume is positive, *i.e.* the reaction quantum yield is reduced if the crystals are elastically compressed along crystallographic axis *b*.[13,18] This unexpected effect is explained by the anisotropy of lattice strain, when the

[a] Institute of Solid State Chemistry and Mechanochemistry SB RAS, Kutateladze Street 18, Novosibirsk, 630128, Russian Federation.
E-mail: eboldyreva@yahoo.com
[b] Novosibirsk State University, Pirogova Street 2, Novosibirsk, 630090, Russian Federation

† Electronic supplementary information (ESI) available: Data characterising diffraction data collection and crystal parameters (Table S1), dependences of the shift of the reflected laser beam *vs.* time at different temperatures (Fig. S1), the change in the distances between the closest NH₃-ligands of the neighbouring complex cations surrounding a selected NO₂-group (Fig. S2), the fragments of the crystal structure with hydrogen bonds (Fig. S3) and the geometries of hydrogen bonds at different temperatures (Table S2). CCDC 1470414–1470434. For ESI and crystallographic data in CIF or other electronic format see DOI: 10.1039/c6ce00840b

total relatively small negative volume change during the reaction (−0.7%) results from a large (+3.9%) expansion along crystallographic axis *b* and a large compression along axes *a* (−2.7%) and *c* (−1.8%) (Fig. 1).[19]

An important parameter that can effect a reaction is temperature. The effect of temperature on the photoisomerisation can be related to both "microscopic" intramolecular processes (dissipation of the excitation energy resulting from a series of radiation-less transitions from the higher to lower energy level in a complex cation), and

Fig. 1 The fragments of the crystal structure of $[Co(NH_3)_5NO_2]Cl(NO_3)$ in different orientations. Chlorine anions are green, Co atoms dark blue, N atoms light blue, and oxygen atoms red. The complex hydrogen bond network (Fig. S3 and Table S2 in the ESI†) is not shown for clarity.

"macroscopic" phenomena related to the anisotropic strain induced in the crystal on temperature variations (expansion on heating, compression on cooling). The "microscopic" and "macroscopic" phenomena are interrelated as the lattice strain on temperature variation results from changes in the anharmonicities of vibrations. Further, structural distortion can have a pronounced effect on the intramolecular transitions between energy states. The problem is very general and is of interest for any photochemical reactions in crystals that are accompanied by structural strain and photomechanical effects.

The rate of photoisomerisation characterises the transition of a compound from the initial state to the final state. Generally, this rate is determined by the transition to the excited state, and the relaxation of the excitation through one or several channels. Temperature can affect any of these stages. If transition to the excited state and radiationless relaxation do not depend on temperature directly, then the effect of temperature on the photoisomerisation is related to the micro- and macro-strain resulting from thermal expansion.

The rate of photoisomerisation of $[Co(NH_3)_5NO_2]X_2$ (X = Cl⁻, Br⁻, I⁻) complexes in the solid state has been reported not to change significantly even at liquid nitrogen[20] and liquid helium[21] temperatures, the activation energy estimated to be 100 cal mol⁻¹.[21] This suggests that the transition to the excited state itself is in fact not thermally activated. It therefore becomes possible to consider the effect of temperature on the photoisomerisation in the crystalline state, focusing on the relation between the rate of photoisomerisation and the anisotropy of lattice strain resulting from temperature variation (thermal expansion on heating or contraction on cooling). It is of particular interest to compare the effect of thermally induced strain with the previously studied effect of strain induced by elastic bending.[11,13,17,18] The values of linear strain in the two cases are comparable, but the anisotropy is different.[15,22,23] Another important difference is that uniform thermal strain does not create any macroscopic stresses in the crystal, in contrast to bending by external loading. A comparison of the effects of the two types of strain on the reaction may give better insight into the role of the crystalline environment in intramolecular photoisomerisation.

The aim of this study was to monitor the kinetics of the photoisomerisation in the crystals of $[Co(NH_3)_5NO_2]Cl(NO_3)$ at multiple temperatures across the range 80–363 K by measuring crystal bending, and to search for correlations between the observed effects and the anisotropic lattice strain induced in the crystals by temperature variations, as measured by single-crystal X-ray diffraction. A study of the temperature dependence of the rate of nitro–nitrito linkage photoisomerisation in $[Co(NH_3)_5NO_2]Cl(NO_3)$ is complicated by the existence of reverse thermal nitrito–nitro isomerisation. In order to overcome this difficulty, we limited the study of the kinetics of photoisomerisation to the initial stage of the transformation where the contribution of the reverse process is negligible.
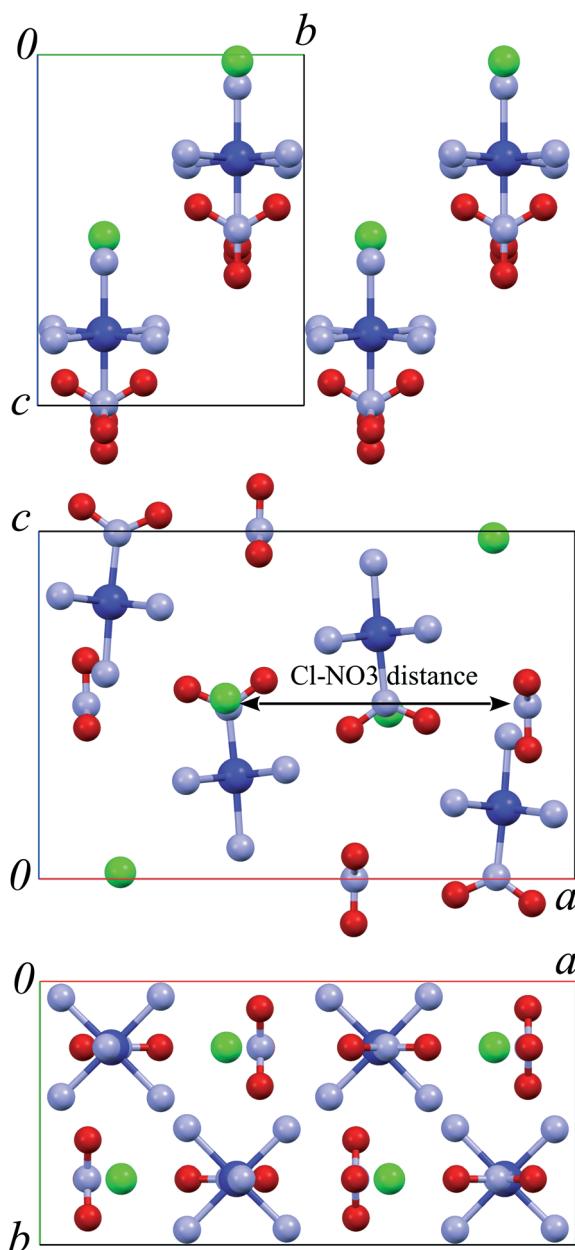
Experimental

Crystals were synthesized and grown as described in ref. 24. To study the kinetics of the photoisomerisation, the experimental set-up described in earlier publications[11,13,17,18] was used. This set-up was modified in such a way so as to enable variable-temperature measurements using a home-made cryo-thermostat (Fig. 2). The crystal was fixed on a copper holder and located in a chamber swept by a stream of dry nitrogen to avoid icing; the temperature of the copper holder was held with a precision better than 1 K over the range 80–373 K. A blue LED (λ = 465 nm, 1 W) was used as the source of excitation radiation. The shift of the free crystal end, resulting from its bending, was monitored by measuring the position of a spot from a laser beam reflected by a mirror (a polished silicon plate) to a point 5 meters away.

The orientation of the crystal with respect to the light source is plotted in Fig. 3. The crystal was irradiated normal to its broad face. Crystal faces were indexed using CrysAlisPro software[25] and 191 reflections were collected with an Oxford Diffraction Gemini R Ultra diffractometer (2D CCD detector, MoKα radiation).

The method requires crystals with a certain thickness. A crystal must be thick enough to enable pasting a mirror to its free end (Fig. 2). At the same time, the crystal must be thin enough so as to not suppress its sensitivity to irradiation. The limit of crystal bending is defined by its breaking point; thicker crystals break significantly earlier than thinner ones on bending.

The range of optimum sizes for this compound is given in Table 1, which sums up the data on the crystals used in this work. The most sensitive measurement could be done for crystal 3. Its thickness was still significantly larger than the characteristic light absorption distance, which is 20 μm.[17,18]
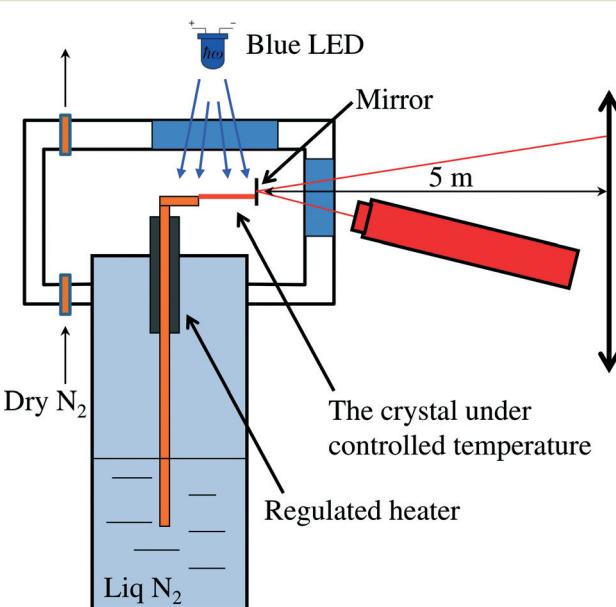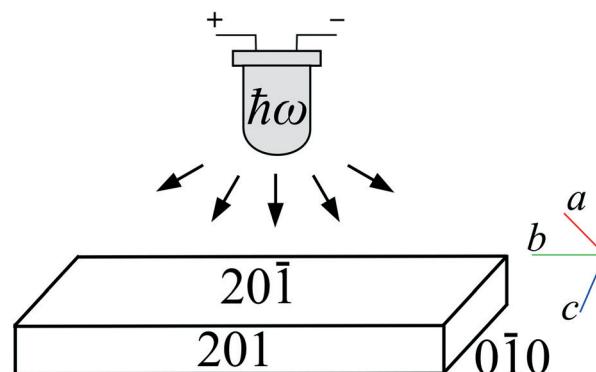

Fig. 3 Orientation of a crystal with respect to the light source. Face indices and directions of crystallographic axes are shown.

This greatly simplified data analysis: all light reaching the crystal surface can be considered to be absorbed by the surface layer.

The bending of a crystal over multiple irradiation/heating (photoisomerisation/reverse thermoisomerisation) cycles was highly reproducible (Fig. 4). This indicates that no irreversible chemical or structural changes (defects) are accumulated in the crystal during these cycles, and there is no fatigue. This makes it possible to use the same crystal for multiple measurements under different conditions (in particular, at different temperatures). This allows one to increase the reliability of the measurements, since data scattering (which would be unavoidable if different crystals were used for the measurements at different temperatures) is eliminated.

Variable-temperature single-crystal X-ray diffraction over the temperature range 100–393 K was carried out using a STOE IPDS-2 diffractometer (MoKα radiation) equipped with an image-plate detector, a graphite monochromator, and an Oxford Cryostream device for temperature control with dry nitrogen flow. At the beginning of the experiment, the sample was heated from 293 K to 393 K in 10 K steps. Subsequently, the sample was cooled directly to 293 K and then X-ray data were collected on cooling to 213 K in 20 K steps, at which point the crystal was covered by ice. The experiment was stopped at 213 K and the sample was heated to evaporate the ice.

After the sample was clear, the temperature was decreased to 193 K and data collection was resumed, obtaining data down to temperatures of 100 K. X-ray data were collected at each temperature point. Cooling and heating rates were ~60 K per hour.

X-AREA and X-RED32 (ref. 26) were used for cell refinement, data collection and data reduction. Crystal structures

Fig. 2 Experimental set-up.

Table 1 Dimensions of the crystals used for measurements

| Crystal	Length, μm	Thickness, μm
1	3230	460
2	5140	730
3	6060	280
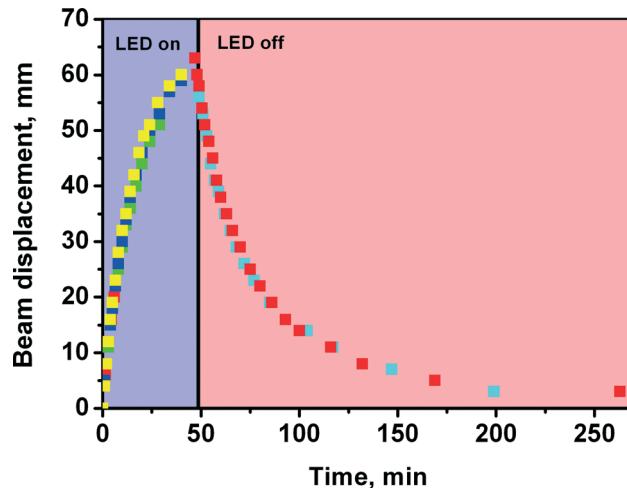
Fig. 4 Illustration of the reproducibility of results over multiple irradiation/heating (photoisomerisation/reverse thermoisomerisation) cycles; crystal #2, T = 363 K. The displacement of the reflected beam on irradiation of the crystal by light from the LED for 50 minutes is shown (rising curve), and that resulting from a subsequent reverse thermoisomerisation in the dark (downward curve).

were solved by direct methods and refined on F^2 using X-STEP32 (ref. 27) and SHELX-2014 (ref. 28) software. All hydrogen atoms were located in the difference Fourier maps; H-atom parameters were treated using HFIX 137 to refine torsion angles in idealized NH_3 groups allowing them to rotate but not to tip. Data characterising data collection and crystal parameters are summarized in Table S1.† All crystallographic data have been deposited with the Cambridge Crystallographic Data Centre.[29–31] Mercury[32] was used for structure visualisation and analysis, including the calculation of voids using the contact surface with a probe radius of 0.9 Å and a grid spacing of 0.2 Å.

Results and discussion

Typical dependences of the shift of the reflected laser beam *vs.* time at different temperatures are plotted in Fig. 5. The full dataset measured at all temperatures is deposited as ESI† (Fig. S1). As the temperature increases, the deviation of the curves from linearity also increases. The non-linearity of crystal bending is a consequence of two main effects: i) the amount of the non-transformed nitro-isomer decreases, and ii) the rate of the reverse nitrito–nitro thermoisomerisation increases as the concentration of the product of the photoisomerisation (nitrito-isomer) increases. One can approximate the time dependence of the photoisomerisation as a function of depth from the surface according to an equation derived in ref. 9:

$$\frac{\partial C}{\partial t} = k_{ph}e^{-\mu x}\left(1 - C\right) - k_{th}C \tag{1}$$

where C – relative local concentration of the reaction product at distance x from the crystal surface, k_{th} – the rate of reverse
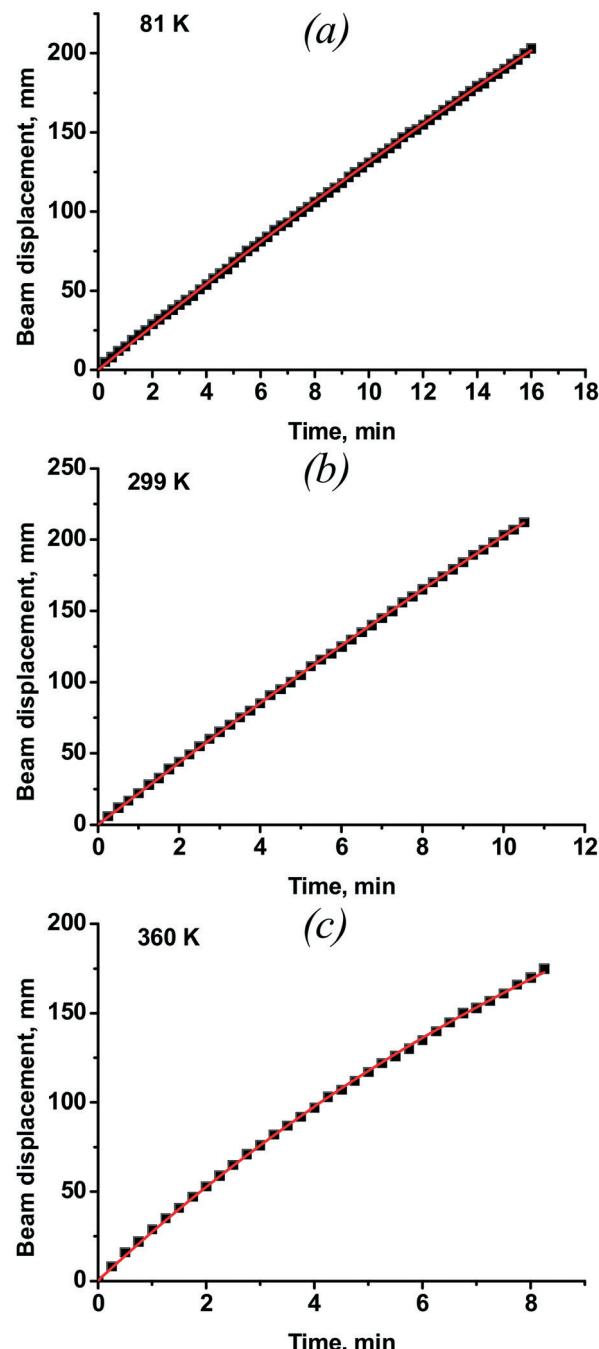
Fig. 5 The displacement of the laser beam during the bending of crystal #3 at variable temperatures: a) 81 K, b) 299 K, c) 360 K (data for other temperatures are available as ESI,† Fig. S1).

thermal reaction, k_{ph} – the rate of photoisomerisation, which can be expressed as $k_{ph} = I_0\alpha\mu v$, where I_0 – flux density of the radiation per unit of the irradiated surface area, α – quantum yield of the photoisomerisation, μ – absorption coefficient in the Beer–Lambert–Bouguer law, v – volume per formula unit of the absorbing substance (μv is extinction of the compound). At low temperature, when k_{th} approaches zero, the reaction slows only because the initial reactant is consumed (transformed), see the first term in eqn (1). As temperature

increases, the contribution of the second term in eqn (1) becomes larger, and the slowing of crystal bending becomes more pronounced.

The value of k_{ph} can be determined from the rate of photoisomerisation at the initial moment, when $C = 0$ in the whole crystal bulk. This corresponds to the calculation of the initial rate of displacement of the reflected laser beam by interpolation of the curves plotted in Fig. 5 to $t = 0$ s. The beam displacement can be related to the geometric parameters of the crystal and experimental set-up (Fig. 2), according to eqn (2):

$$\Delta x = \frac{2LB}{R} \tag{2}$$

where L – crystal length, B – the distance from the mirror reflecting the beam to the scale, R – curvature radius of the bent crystal, which is calculated as described in ref. 9 by eqn (3):

$$\frac{1}{R} = \frac{12\varepsilon}{h^3}\int_0^h \left(\frac{h}{2} - x\right) C(x)\,dx \tag{3}$$

h – crystal thickness, ε – relative elongation of the crystal along the long axis corresponding to complete transformation (0.039 in our case). The initial rate of displacement of the laser beam can then be expressed as

$$\left(\frac{\Delta x}{\Delta t}\right)_{t=0} \approx \frac{k_{ph}}{\mu}\times\left[\frac{12LB\varepsilon}{h^2}\left(1 - \frac{2}{\mu h}\right)\right] \tag{4}$$

Eqn (4) takes into account that the crystal thickness is much more than the characteristic radiation absorption depth μ^{-1}. This makes it possible to directly calculate the value of k_{ph}. This constant is present in eqn (4) via the relation $k_{ph}/\mu = I_0\alpha v$. This means that the only value that can contribute significantly to the temperature dependence of the measured rate of crystal bending is the quantum yield of the photo-transformation, α.

The temperature dependence of the rate of photoisomerisation k_{ph} is plotted in Fig. 6a. It is apparent that a less than two-fold change in the quantum yield, corresponding to a temperature change of almost 300 K, cannot correspond to a thermally activated process. As suggested initially, this can only be related to the effect of thermally induced lattice strain. Relative changes in the rate of photoisomerisation on temperature variation are comparable in value to that on elastic bending by external loading, if the corresponding lattice strain is of the same order of magnitude. This fact additionally supports the hypothesis that lattice strain makes the largest contribution to the temperature dependence of the photoisomerisation rate in a crystal. In the case of external loading, it was logical to seek a correlation between the quantum yield and lattice strain in one selected direction, namely, along the long axis of the crystal. In contrast, in the case of thermal strain, the choice of a selected direction is not so obvious a priori. Uniform thermal strain does not cause any
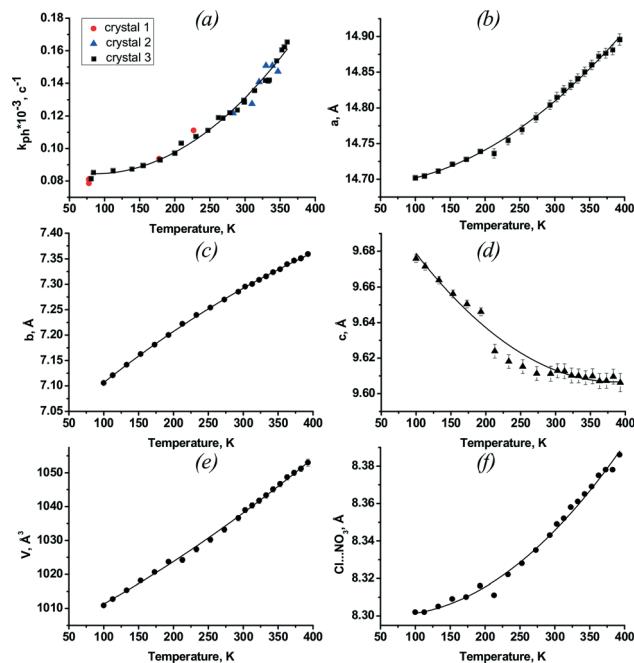
Fig. 6 The temperature dependences of: a) the rate constant of photoisomerisation k_{ph}; b–e) unit cell parameters a, b, c and volume V; f) the distance between the anions Cl and NO_3, surrounding a nitro-ligand NO_2 (see Fig. 1).

macroscopic stress and is anisotropic. Generally, all components of the strain tensor and their possible combinations should be considered as potentially correlating with the rate of photoreaction.

Since the dependence of quantum yield on strain in experiments with external loading of the crystal was linear,[11,13,17,18] it also seemed logical to look for the strain tensor components that linearly correlate with the rate of photoreaction in the case of thermally induced strain. The temperature dependences of the unit cell parameters and volume are plotted in Fig. 6b–e. It is clear that only the shape of the $a(T)$ curve resembles that of the temperature dependence of the photoisomerisation rate constant.

Although there is a qualitative correlation between the direction of change of the reaction rate, on the one hand, and the cell volume or the volume of the "voids" around the nitro group, on the other hand, their quantitative changes are not linearly correlated (Fig. 1 and 7). The dependences of the cell volume and void volume on temperature are practically linear (Fig. 6e and 7), whereas the magnitude of the gradient of $k_{ph}(T)$ decreases at lower temperatures (Fig. 6f).

The existence of a formal correlation between the reaction rate constant and lattice strain can be rationalised using the concept of a reaction cavity.[13,33–35] A reaction cavity is defined as the free space in the crystalline environment that immediately surrounds a reacting molecule or molecular fragment. The simplest approximation is to consider the reaction cavity as being rigid (i.e. constant over the course of the reaction) and to seek correlations between the size of a reaction

Fig. 7 Volume of voids surrounding the nitro-ligand in the structure of [Co(NH$_3$)$_5$NO$_2$]Cl(NO$_3$) vs. temperature. Void shape (yellow) and its position between ligands are shown.

Fig. 8 The correlation between the rate of photoisomerisation and the distance between the anions Cl and NO$_3$, surrounding a nitro-ligand NO$_2$ (see Fig. 1).

NO$_3^-$ (Fig. 1, 6f and 8). The correlation can be approximated by eqn (5):

$$k_{ph}(T) = k_{ph}(363\ \text{K}) \times \left(1 + q\frac{l(T) - l(363\ \text{K})}{l(363\ \text{K})} \right) \qquad (5)$$

where $l(T)$ is the temperature-dependent Cl–NO$_3$ distance. The coefficient of linear correlation q is equal to 55 ± 5, and is close to the value of the similarly defined parameter q = 40.[13,18] The exact mechanism that underpins the effect of the a parameter and the Cl$^-$–NO$_3^-$ (and NO$_2$–NH$_3$) distance on the reaction rate when considering thermal strain requires further study. It can be preliminarily interpreted in terms of coupling between selected anharmonic vibrational modes, electronic photoexcitation and the motion of the nitro-ligand, resulting in the change of its orientation in the crystal structure and bonding to Co-atom.

Remarkably, in neither the case of external elastic compression nor thermally induced strain does the reaction rate correlate with lattice strain along the crystallographic c direction (Fig. 1 and 7). Instead, lattice expansion along c that takes place on both cooling (in this work) and on elastic compression of the b axis[23] corresponds to a *decrease* in the reaction rate.

One can suppose that the apparently different effects of macroscopic strain on the photoisomerisation rate in the two cases – external elastic compression and thermal strain – are in fact rooted in identical phenomena. This becomes evident if the microscopic stress experienced by the excited state of the complex cation on irradiation is considered. The macroscopic thermal strain can be suggested to subject the excited state to microscopic stress mainly along the a axis. In contrast, direct external loading of the crystal appears to result in microscopic stress mainly along the b axis. No significant microscopic stress arises along c, presumably, since enough free space is present in this direction in the starting crystal

cavity and the reaction rate. Such an approach is often helpful when a series of related compounds are compared.[13,14,33] Qualitatively, the free volume that is available in the starting crystal correlates with the rate of photoisomerisation in Co(III) compounds: the larger the reaction cavity, the larger the reaction rate constant.[13,14] However, further analysis of the anisotropic lattice strain resulting from the reaction itself (when considering a "flexible" reaction cavity[34,35]) reveals finer details that are not obvious *a priori*.

If strain is induced by external load, the reaction rate correlates quantitatively with compression along the crystallographic b direction.[11,13,14,17] This can be rationalised if one considers the anisotropy of lattice strain resulting from the reaction. As a result of photoisomerisation the structure expands along b, and thus compression along this direction by an external load is not favourable for the reaction.[11,13,14]

If strain results from temperature variations (as in this work), then the reaction rate correlates with changes along the crystallographic a direction. This effect can be rationalised if one considers the crystal packing. It is logical to start the analysis by considering NH⋯O hydrogen bonds between the nitro-group that is directly involved in the photoisomerisation, and the amino-groups of the neighbouring complex cations (Fig. S2†). The change in distance between a select NO$_2$-group and its nearest NH$_3$-ligands (Fig. 1 and Fig. S2†) is qualitatively similar to $a(T)$ and can be correlated with the rate of photoreaction.

Correlating more closely with the rate of photoreaction is the temperature-dependent interatomic distance between the two anions that surround each nitro-ligand, namely Cl$^-$ and

structure, and is preserved over the course of isomerisation. Further investigation into the lattice dynamics of this system may shed more light on the microscopic stresses that arise over the course of the reaction at various temperatures and on elastic compression.

Conclusions

The phenomenon of bending a crystal on irradiation (a photomechanical effect, or photobending) is more than a curious observation. These effects have considerable practical applications in supramolecular devices, *e.g.* sensors and actuators. Macroscopic strain can be measured quantitatively with high precision and reproducibility. These data can be used to obtain an insight into the microscopic mechanism of the transformation and the effect of crystalline environment on the intramolecular photorearrangement.

The rate of photoisomerisation in $[Co(NH_3)_5NO_2]ClNO_3$ correlates clearly with lattice strain, be this strain induced by external elastic loading or by thermal expansion/contraction. At the same time, in the case of external loading the rate of the photoreaction correlates with strain along the long crystal axis (b), whereas in the case of thermal strain the correlation is with changes normal to the long crystal axis, *i.e.* within the irradiated plane (parameter a). This can be rationalised by assuming that selected lattice vibrations are coupled with photoexcitation. Intramolecular motions are important when strain results from heating/cooling and is not associated with any macroscopic mechanical stresses.

A very interesting fact is that the value of the q parameter, characterising the dependence of the photoisomerisation rate on lattice strain, is high both in the case of external elastic loading and on temperature-induced strain (40 (ref. 17 and 18) and 50 (this work), respectively). This means that the yield of the intramolecular photoisomerisation is highly sensitive to even relatively small distortions of the crystalline environment. This is a manifestation of the large role of feedback phenomena in solid-state photochemical reactions, which are similar in this respect with other types of solid-state transformations.[13,36]

Acknowledgements

Notes and references

1 G. A. Abakumov and V. I. Nevodchikov, *Dokl. Akad. Nauk SSSR*, 1982, **266**, 1407.
2 E. V. Boldyreva, A. A. Sidelnikov, A. P. Chupakhin, N. Z. Lyakhov and V. V. Boldyrev, *Dokl. Akad. Nauk SSSR*, 1984, **277**, 893.
3 F. I. Ivanov and N. A. Urban, *React. Solids*, 1986, **1**, 165.

4 M. Irie, *Chem. Rev.*, 2000, **100**, 1685.
5 H. J. Shepherd, I. A. Gural'skiy, C. M. Quintero, S. Tricard, L. Salmon, G. Molnár and A. Bousseksou, *Nat. Commun.*, 2013, **4**, 2607, DOI: 10.1038/ncomms3607.
6 N. K. Nath, M. K. Panda, S. C. Sahoo and P. Naumov, *CrystEngComm*, 2014, **16**, 1850.
7 M. Irie, T. Fukaminato, K. Matsuda and S. Kobatake, *Chem. Rev.*, 2014, **114**, 12174.
8 T. Kim, L. Zhu, R. O. Al-Kaysi and C. J. Bardeen, *ChemPhysChem*, 2014, **15**, 400.
9 P. Naumov, S. Chizhik, M. K. Panda, N. K. Nath and E. Boldyreva, *Chem. Rev.*, 2015, **115**, 12440.
10 M. D. Manrique-Juárez, S. Rat, L. Salmon, G. Molnár, C. M. Quintero, L. Nicu and H. J. Shepherd, *Coord. Chem. Rev.*, 2016, **308**, 395.
11 E. V. Boldyreva, *Mol. Cryst. Liq. Cryst. Inc. Nonlinear Opt.*, 1994, **242**, 17.
12 N. Masciocchi, A. N. Kolyshev, V. E. Dulepov, E. V. Boldyreva and A. Sironi, *Inorg. Chem.*, 1994, **33**, 2579.
13 *Reactivity of Molecular Solids, Molecular Solid State Series*, ed. E. V. Boldyreva and V. V. Boldyrev, Wiley, 1999, vol. 3, p. 328.
14 E. V. Boldyreva, *Russ. J. Coord. Chem.*, 2001, **27**, 297.
15 P. Naumov, S. C. Sahoo, B. A. Zakharov and E. V. Boldyreva, *Angew. Chem.*, 2013, **252**, 9990.
16 B. A. Zakharov, A. S. Marchuk and E. V. Boldyreva, *CrystEngComm*, 2015, **17**, 8812.
17 E. V. Boldyreva and A. A. Sidelnikov, *Izv. Sib. Otd. Akad. Nauk SSR, Ser. Khim. Nauk*, 1987, **5**, 139.
18 B. I. Yakobson, E. V. Boldyreva and A. A. Sidelnikov, *Izv. Sib. Otd. Akad. Nauk SSR, Ser. Khim. Nauk*, 1989, **1**, 6.
19 E. V. Boldyreva, A. V. Virovets, L. P. Burleva, V. E. Dulepov and N. V. Podberezskaya, *Zh. Strukt. Khim.*, 1993, **34**, 128.
20 D. A. Johnson and K. A. Pashman, *Inorg. Nucl. Chem. Lett.*, 1975, **11**, 23.
21 E. J. Rose and D. S. McClure, *J. Photochem.*, 1981, **17**, 171.
22 E. V. Boldyreva, J. Kivikoski and J. A. K. Howard, *Acta Crystallogr., Sect. B: Struct. Sci.*, 1997, **53**, 394.
23 E. V. Boldyreva, H. Ahsbahs and H. Uchtmann, *Ber. Bunsen-Ges.*, 1994, **98**, 738.
24 E. V. Boldyreva, J. Kivikoski and J. A. K. Howard, *Acta Crystallogr., Sect. B: Struct. Sci.*, 1997, **53**, 394.
25 *Oxford Diffraction. CrysAlisPro*, Oxford Diffraction Ltd, Abington, England, 2010.
26 *Stoe & Cie. X-AREA and X-RED32*, Stoe & Cie, Darmstadt, Germany, 2006.
27 *X-STEP*, Stoe&Cie, Darmstadt, Germany, 2000.
28 G. M. Sheldrick, *Acta Crystallogr., Sect. C: Struct. Chem.*, 2015, **71**, 3.
29 F. H. Allen, *Acta Crystallogr., Sect. B: Struct. Sci.*, 2002, **58**, 380.
30 C. H. Görbitz, *Acta Crystallogr., Sect. B: Struct. Sci., Cryst. Eng. Mater.*, 2016, **72**, 167.
31 C. R. Groom, I. J. Bruno, M. P. Lightfoot and S. C. Ward, *Acta Crystallogr., Sect. B: Struct. Sci., Cryst. Eng. Mater.*, 2016, **72**, 171.

32 C. F. Macrae, P. R. Edgington, P. McCabe, E. Pidcock, G. P. Shields, R. Taylor, M. Towler and J. van de Streek, *J. Appl. Crystallogr.*, 2006, **39**, 453.

33 Y. Ohashi, *Crystalline State Photoreactions*, Springer, 2014, p. 208.

34 T. Luty and C. J. Eckhardt, *J. Am. Chem. Soc.*, 1995, **117**, 2441.

35 E. V. Boldyreva, *Solid State Ionics*, 1997, **101**–**103**, 843.

36 A. P. Chupakhin, A. A. Sidel'nikov and V. V. Boldyrev, *React. Solids*, 1987, **3**, 1.